5ICEGE
5th International Conference on Earthquake Geotechnical Engineering
January 2011, 10-13 | Santiago, Chile
Paper No. SRSTT

SITE RESPONSE STUDIES ON EXTREME VERTICAL GROUND MOTIONS BEYOND 1G

Tetsuo TOBITA [1], Susumu IAI[2], Tomotaka IWATA[3], Shin AOI[4] , Koji HADA[5]

ABSTRACT

An unprecedented vertical surface peak ground acceleration of nearly four times of gravity, more than twice of its horizontal ones was recorded at the KiK-net, IWTH25 vertical array site during the 2008 Iwate-Miyagi Nairiku, Japan, earthquake (Mw 6.9) (Aoi et al., Science, 2009). Waveform of the vertical acceleration shows a clear asymmetric form, which has large amplitude in upward direction. To study this recently discovered nonlinear behavior of the surface ground motion, analyses based on numerical and physical modeling are conducted. For numerical analysis, finite element method with parameters derived from the borehole data at the IWTH25 station is conducted. The numerical analysis successfully simulates the asymmetric vertical motion recorded at the IWTH25 station. Numerical analysis with simple condition, homogeneous 10 m layer with vertical sinusoidal input motion, reveals that the asymmetric motion is a combination of the lower bound of negative acceleration due to gravity and larger positive pulses due to the compression (vertical) stress induced in the ground. Asymmetric vertical wave forms are reproduced with physical model tests under 1G condition in which sinusoidal vertical input motion is given to 1 m thick dry sand layer. Measured vertical acceleration is significantly similar to the ones obtained by the numerical analysis. This validates the use of the numerical method employed in the present study.

Keywords: Numerical modeling, Physical modeling, Vertical motion, the 2008 Iwate-Miyagi, Japan, earthquake, Strong motion

INTRODUCTION

Nonlinear dynamic response is one of the distinguishing characteristics of the ground under strong shaking. The nonlinearity has been reported and investigated by many researchers for more than 40 years. The investigation has been mainly concerned with the following two subjects:

1. The shift of the predominant frequency toward lower frequencies and the decrease of peak amplitudes of acceleration [e.g., Idriss and Seed (1968), Idriss (1990)].
2. High spikes on horizontal acceleration time histories due to cyclic mobility in relatively dense sand deposit [e.g., the 1987 Superstition Hills earthquake (Holzer et al. 1989); the 1993 Kushiro-oki, Japan, earthquake (Iai et al. 1995); the 1994 Northridge earthquake (Bardet and Davis 1996); the 1995 Hyogoken Nanbu, Japan, earthquake (Iwasaki and Tai 1996); the 2001 Nisqually earthquake (Frankel et al. 2002); the 2007 Niigataken Chutsu-oki, Japan, earthquake (Kayan et al. 2009)].

[1] Assistant Professor, Disaster Prevention Research Institute, Kyoto University, Gokasho, Uji, Kyoto 611-0011, Japan, tobita@geotech.dpri.kyoto-u.ac.jp
[2] Professor, Disaster Prevention Research Institute, Kyoto University.
[3] Professor, Disaster Prevention Research Institute, Kyoto University.
[4] Senior Researcher, National Research Institute for Earth Science and Disaster Prevention.
[5] NEWJEC Inc..

In addition to the above-mentioned two types of nonlinear response of the ground, the third nonlinearity under strong ground motion has been recently discovered as being asymmetric form of the surface vertical acceleration amplitude (Aoi et al. 2008). In the 2008 Iwate-Miyagi Nairiku, Japan, earthquake, a very large acceleration amplitude that exceeded 40 m/s^2 (three components combined) was recorded (Fig. 1) at the KiK-net, IWTH25 vertical array station. The site is located about 3 km southwest of the epicenter on the hanging wall of the source fault. The earthquake was caused by the inland reverse fault with a 30 km strike and 20 km depth. At the IWTH25 station, three-component seismometers are installed at the surface and G.L. – 260 m, forming a vertical array. The site is located in a volcanic region, and locally it is on the river sediments underlain by igneous rocks, such as tuff. The recorded wave form of the surface vertical acceleration has large amplitude only in the positive direction. The maximum amplitude of vertical acceleration is four times larger than the acceleration of gravity and two times larger than its horizontal components. Aoi et al. (2008) reported and qualitatively explained the mechanism of this phenomenon by the analogy of bouncing a piece of matter on a trampoline, and they called it the "trampoline effect."

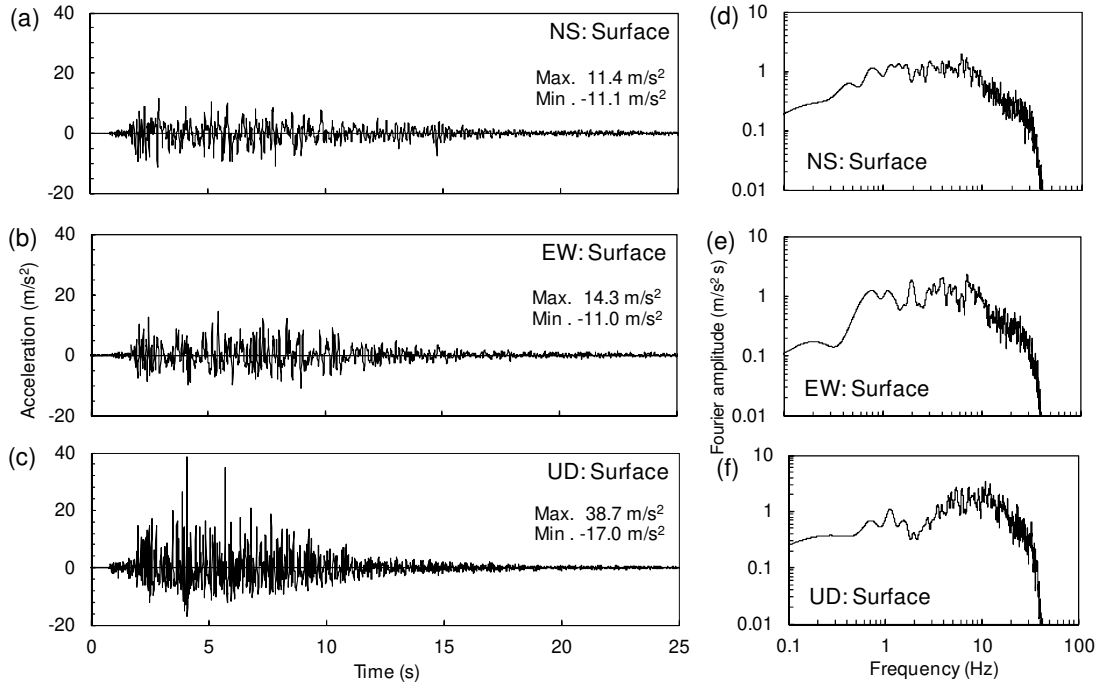

Figure 1. Measured time histories and Fourier amplitudes of surface acceleration at IWTH25 after the 2008 Iwate-Miyagi Nairiku, Japan, earthquake. Asymmetric amplitude appears on the UD record.

The asymmetric form may be attributed to physical characteristics of granular media, which show asymmetric response against normal compression and tension force. That is, granular media, such as dry sands, have less resistance against tension force. Yamada et al. (2009) analyzed the asymmetric motion recorded in the 2008 Iwate-Miyagi Nairiku earthquake with records of other earthquakes and nuclear explosions whose vertical PGA showed greater than 1 g. They found that vertical acceleration records whose maximum amplitude is greater than 1 g tend to have larger positive amplitude than that of the negative amplitude, and negative amplitude is bounded at about - 1 g. They also estimated the thickness

of the spalled layer to be 30 to 60 m with the amount of separation 1 to 12 mm during the 2008 Iwate-Miyagi Nairiku earthquake using the periods of spikes (Eisler and Chilton 1964).

Tobita et al (2010) conducted the numerical study whose results are partially presented in this paper. In addition to what they have reported, results obtained by the physical model testing of the ground response against vertical motion are presented.

ANALYTICAL MODEL

In this study, the multiple simple shear mechanism proposed by Towhata and Ishihara (1985) and Iai, et al. (1992) is implemented. The model is formulated based on the concept of contact forces in granular media, which is thought to be suitable for the study of the asymmetric vertical motion, because the motion might be intrinsically generated by the nature of granular or discrete media.

Model Behavior Under Normal Compression and Tension Stresses.

The finite-element code called FLIP (Iai et al. 1992) is implemented for nonlinear site response analysis. Total stress analysis is conducted—i.e., there is no excess pore water pressure buildup during shaking. The code utilizes the multiple simple shear mechanism as the nonlinear constitutive relation (Towhata and Ishihara 1985). In this model, contact forces between sand particles are idealized by evenly distributed multiple springs, whose property is characterized by the hyperbolic type. The model automatically accommodates the principal stress rotation, which plays an important role in the cyclic behavior of anisotropically consolidated sands. In the finite-element code, FLIP, if the volumetric strain is positive, then all of the stress components are set to be zero, i.e.,

$$(\varepsilon_x + \varepsilon_y) - \varepsilon_p \geq 0 \quad \text{(Tension), then} \quad \sigma_x' = \sigma_y' = \tau_{xy}' = 0 \tag{1}$$

As will be shown in the next section, this is the property that simulates asymmetric behavior of granular media with no cohesion.

Behavior of the multiple simple shear model is investigated by applying vertical compression and tension forces to a single element (Fig. 2). Model parameters for this particular study are: shear modulus = 3.2×10^5 (kPa), Poisson's ratio = 0.33, density = 1.8 (t/m^3), and friction angle = 35°. Computation was carried out under drained condition. For both strains and stresses, tension is taken as positive. First, the element is isotropically consolidated with stress $\sigma_0 = -49$ (kPa), which is equivalent to the confining stress at shallow depth about 2.8 m, with nodal constraints illustrated in Fig. 2(a). Then, it is stretched and compressed vertically by enforcing cyclic normal force to nodes 3 and 4 [Fig. 2(b)]. Here, the horizontal displacements of nodes 3 and 4 are constrained. The analytical time step of $\Delta t = 10^{-4}$ was employed. The wilson's theta method with $\theta = 1.4$ is utilized for the numerical integration scheme. Figure 3(a) depicts time histories of mean stress, $\sigma_m = (\sigma_x + \sigma_y)/2$, and volumetric strain, $\varepsilon_v = \varepsilon_x + \varepsilon_y$, on the left and right vertical axes, respectively. As shown in Fig. 3(a), when the mean stress is zero, tensile strain abruptly increases; that is, the element is vertically stretched. The stress-strain curve in Fig. 3(b) gives another view of this property. Namely, the curve starts at the point indicated as "1" in Fig. 3, where mean stress is – 49 kPa, then it is gradually stretched, and once the mean stress reaches zero at "2", volumetric strain abruptly increases up to about 0.3%. On the compression side, in the given range of enforced vertical stress, the stress-strain relationship is within an elastic range following the line whose slope is defined by the rebound modulus of $K = 605$ MPa.

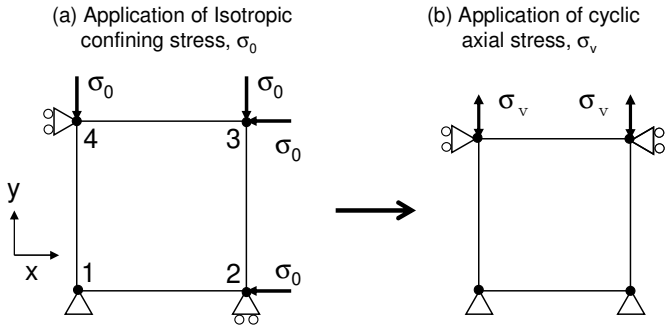

Figure 2. Illustration for application of isotropic confining pressure (a) and cyclic axial stress (b) to a single element.

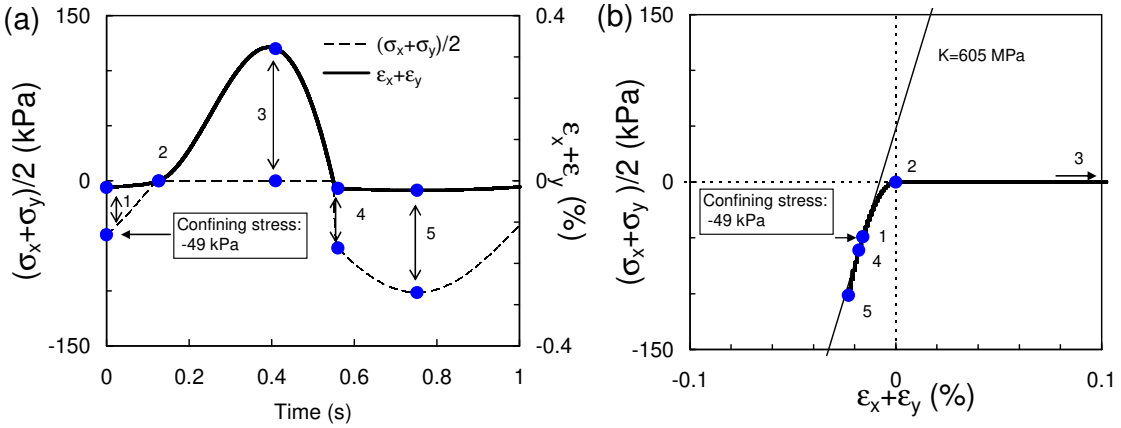

Figure 3. Time histories of (a) mean stress and volumetric strain, and (b) mean stress versus volumetric strain curve.

Numerical Analysis for Measured Earthquake

Model Parameters for Site Response Analysis of KiK-net, IWTH25 Station.
Physical model parameters, such as shear modulus and poisson's ratios, are estimated from the PS velocity profile obtained at the KiK-net, IWTH25 station. Table 1 summarizes model parameters implemented in the following analysis. Based on the velocity profile (NIED 2010), the model ground is divided into 8 layers from the surface to G.L. – 260 m. The borehole profile deeper than 120 m shows that the tuff, whose S wave velocity exceeds 1,300 m/s, is predominant. Above it, mud stones and terrace deposit constitute the layers. Densities of material are given as follows: 2.2 t/m^3 for surface cover soil, 2.3 t/m^3 for sediments, and tuff and mud stones are set uniformly at 2.6 t/m^3 (Toyota 2009).

In the analysis, the ground is modeled with single-column elements (251 elements) whose width is 1 m, and height varies from 0.86 m (layer 1) to 1.09 m (layer 7). With this model ground, the frequency component of the maximum 100 Hz can be properly simulated. The observed horizontal and vertical accelerations at the base are given as input accelerations without de-convolution of up-coming and down-going waves.

Table 1. Model Parameter of the ground profile at the KiK-net, IWTH25 Station

Layer No.	Depth of bottom of layer	Wave velocity		Density	Poisson's ratio	Shear modulus	Bulk moduls	Reference confining stress		Friction angle	Rayleigh damping factor: β
		P	S	ρ	v	G	K	σ_r'	h_{max}		
	(m)	(m/s)	(m/s)	(t/m^3)		(kPa)	(kPa)	(kPa)		(deg.)	
1	6.00	850.0	430.0	2.2	0.33	406780	1047127	9.9			
2	34.0	1770	530.0	2.3	0.45	646070	6344243	58.2			
3	64.0	2310	680.0	2.6	0.45	1183282	12077371	115.8			
4	112	2310	1120	2.6	0.35	3252659	9499628	209.1	0.2	45	0.0015
5	175	4010	1780	2.6	0.38	8107936	30338395	330.0			
6	204	2620	1380	2.6	0.31	4873360	11068187	385.7			
7	242	3180	1810	2.6	0.26	8383540	14699578	458.6			
8	260	3180	1810	2.6	0.26	8383540	14699578	493.2			

Site Response Analysis for the 2008 Iwate-Miyagi Nairiku, Japan, Earthquake

Site response analysis is conducted to simulate asymmetric vertical motion observed in the 2008 Iwate-Miyagi Nairiku, Japan, earthquake. Measured input motion of both horizontal (NS) and vertical (UD) components at the base of the KiK-net array at IWTH25 [Figs. 4(c) and (f)] was input at the base of the model ground with a time step of 0.01 s, which was the same time step as the measured acceleration. Figure 4 compares measured and computed surface accelerations. Coherencies between these accelerations in a range of 0 to 25 Hz for NS and UD components are, respectively, 0.10 and 0.26 on average. As shown in Figs. 4(d) and (e), the computed surface acceleration has an asymmetric shape in the vertical component as with the measured one—i.e., positive spikes and bounded negative amplitude. The maximum amplitude of measured vertical acceleration was about 38.7 m/s^2, while the one computed over-estimates to be about 61.2 m/s^2. Negative amplitudes of surface vertical acceleration show, on average, significant agreements between observation and analysis, and it is close to the acceleration due to gravity. This might indicate the temporal free-fall of the ground. As seen in Fig. 4(a), amplitude of computed horizontal acceleration is smaller than that of the measured. Although the maximum amplitude computed is larger than the observed, overall amplitude in computation is small. This may be due to the strong vertical motion under which the transmission of the shear wave is prevented by the low confining stress induced in the element.

The maximum tensile vertical ground displacement computed by multiplying the vertical strains of elements in tension to the thickness of the elements is 6.2 mm at 3.50 s when the elements down to G.L. – 111 m are in tension [Fig. 5(a)]. The maximum vertical acceleration at the ground surface appears at 3.57 s just after the occurrence of the maximum tensile vertical displacement. The value of maximum tensile displacement, 6.2 mm, is somehow comparable with those obtained by Yamada et al. (2009). They obtained the amount of separation between layers to be 1 to 12 mm by the simple computation method (Eisler and Chilton 1964). However, they estimated the thickness of the separated layer, or depth of separation, to be 30 to 60 m which is about half of the thickness of the ground elements in tension obtained in this study (111 m). As shown in Fig. 5(b), levels of the tensile vertical displacement in each element vary with depth and time. This indicates that the ground is not bouncing as a block, but stretched at certain amounts determined by the physical properties of each layer. Tensile displacements exerted in elements near the ground surface are decreasing. This may be because of the lack of elements which pull the surface elements upwardly.

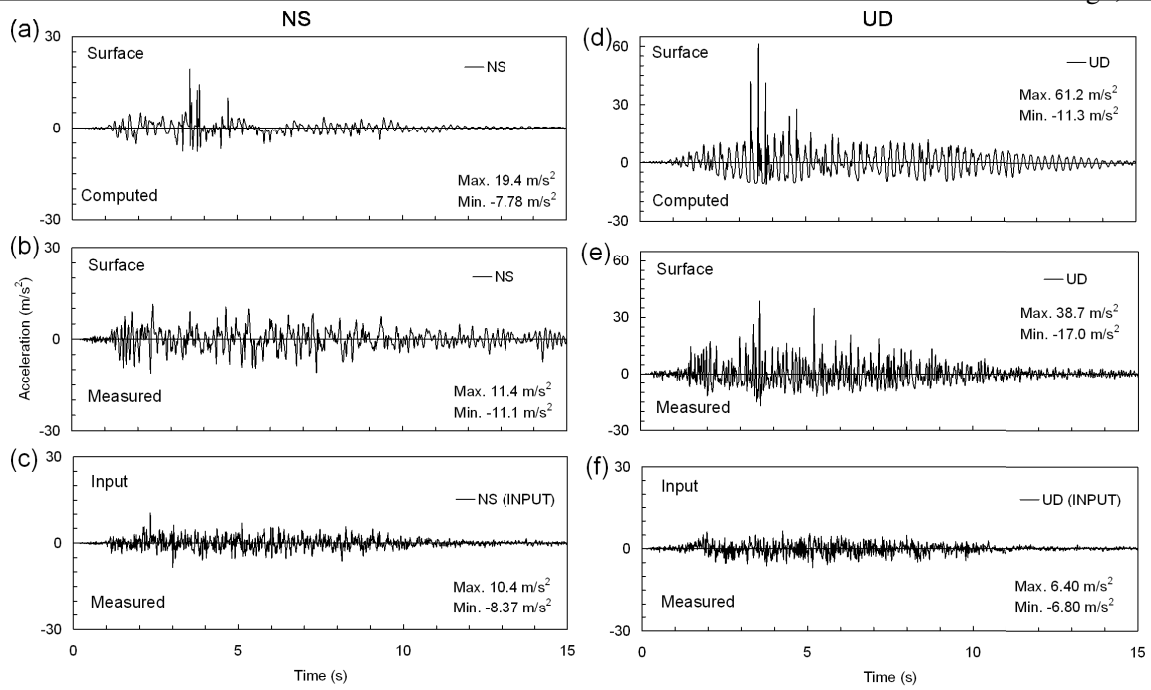

Figure 4. Measured and computed surface acceleration (NS and UD components) for the 2008 Iwate-Miyagi Nairiku earthquake.

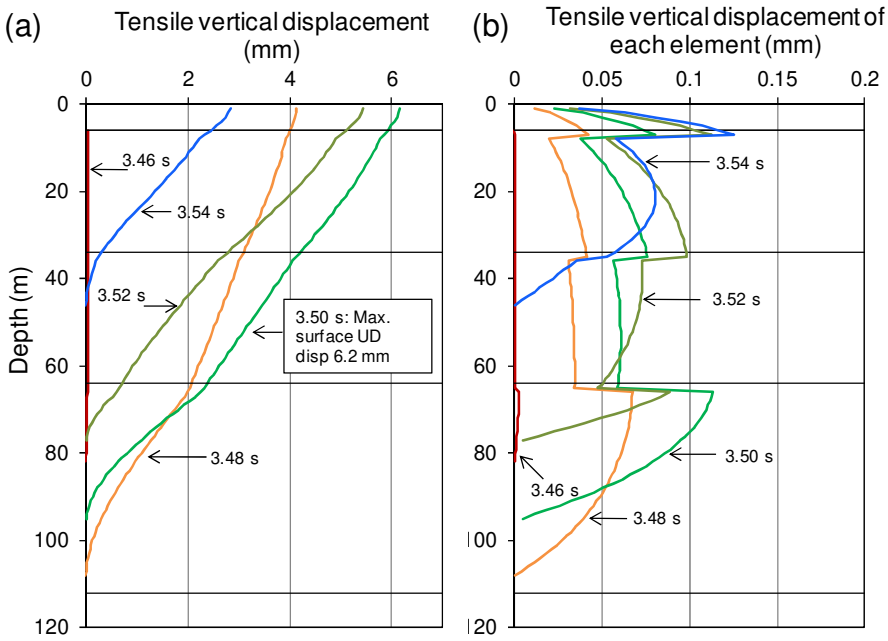

Figure 5 Computed tensile vertical displacements from 3.46 s to 3.54 s: (a) tensile vertical displacement, (b) tensile vertical displacement exerted in each element.

Numerical Analysis Under Simple Condition.

To study the asymmetric vertical ground motion under simple condition, a column 10 m deep with 20 elements is implemented. Each mesh is a square with 0.5 m on a side. The displacement degrees of

freedom at the bottom nodes are fixed in both horizontal and vertical directions. To simulate infinite half-space ground motion, a pair of nodes at the same depth is constrained to have the same displacement degree of freedom in both horizontal and vertical directions. Thus, in the computation, degrees of freedom at each node, except for the bottom nodes, are two (horizontal and vertical), while material parameters vary with depth. The input acceleration is given at the base nodes. Analysis is carried out by assuming dry conditions. Sinusoidal input acceleration with 10 Hz and the amplitude of 19.6 m/s^2 (= 2 g) is given at the base of the model. In this study, only the vertical motion is given. A computational time step of $\Delta t = 0.001$ (s) was employed.

As shown in Fig. 6, time history of the surface vertical acceleration has a characteristic shape, i.e., positive pulses and nearly flat negative amplitudes. Generation of this wave form can be explained as follows.
(1) Compression: Surface acceleration starts to abruptly increase (indicated by (1) in Fig. 6) when the input vertical motion becomes lower than 9.8 m/s^2. Positive pulses may be the result of compression force generated in the element as reaction against collision with the elements underneath. This compression force creates an acceleration pulse in the upward direction. Small upward pulses just after the first large pulses [seen clearly in Fig. 6(b)] may be due to bouncing of the element after the first collision. At this stage, both the input and surface accelerations are oriented in the negative direction, and also the volumetric strain of the surface element shown in Fig. 6(a) is negative (compression).
(2) Tension: Nearly flat amplitude of surface negative acceleration appears when the input acceleration is close to the absolute minimum. After this stage, due to the repulsion force accumulated in the element, slight reduction of downward acceleration may cause extension of the surface element ($\varepsilon_v > 0$).

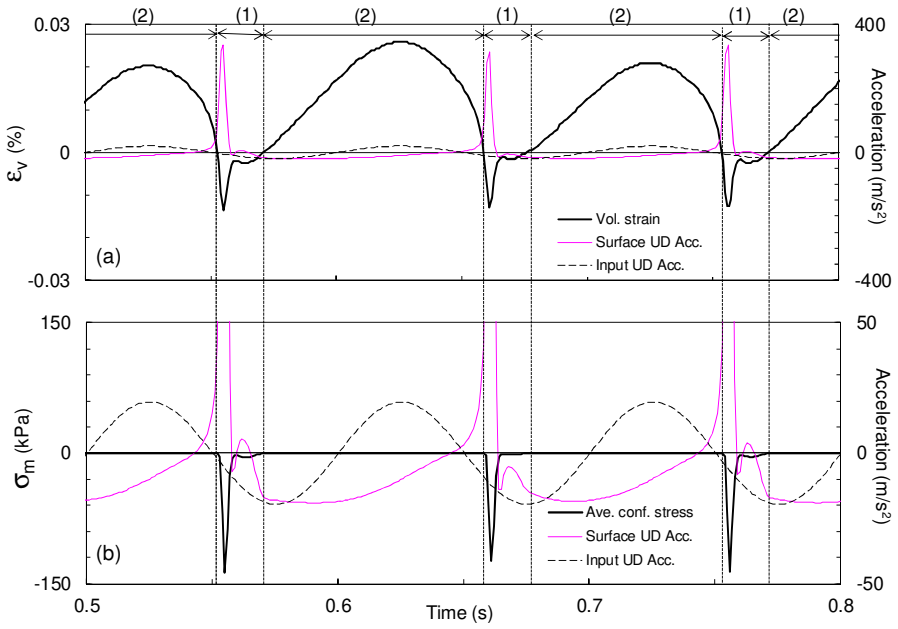

Figure 6. Time histories of (a) volumetric strain, vertical input, and vertical surface acceleration, (b) mean stress, vertical input, and vertical surface acceleration of the surface element. The scale of acceleration in (b) is magnified eight times that of (a). At the top figure, (1) denotes elements is in "Compression" and (2) "Tension"

These steps are repeated for the sinusoidal input motion. Input acceleration amplitude of – 2 g may be unrealistic. However, this example clearly shows that the lower bound of surface acceleration is

controlled by the input acceleration. In reality, the surface vertical wave form may be affected not only by the amplitude but also frequency of input acceleration. The effect of input frequency in conjunction with natural frequency of the ground is considered later in physical model testing.

Figure 7 shows time histories of the input and surface accelerations (right axis) for the cases of (a) 19.6 m/s^2 and (b) 9.8 m/s^2. In Fig. 7, horizontal solid markers indicate the duration of extension of an element at a certain depth (left axis). When the amplitude of input acceleration is 2 g [Fig. 7(a)], tensile volumetric strains are generated as deep as 10 m, and the duration of tension is much longer than that of compression. When the amplitude of input acceleration is 1 g [Fig. 7(b)], the duration of tension is much shorter, and only the elements whose depth is shallower than G.L. – 4 m are in the tensile state after the 3rd cycle of the input motion.

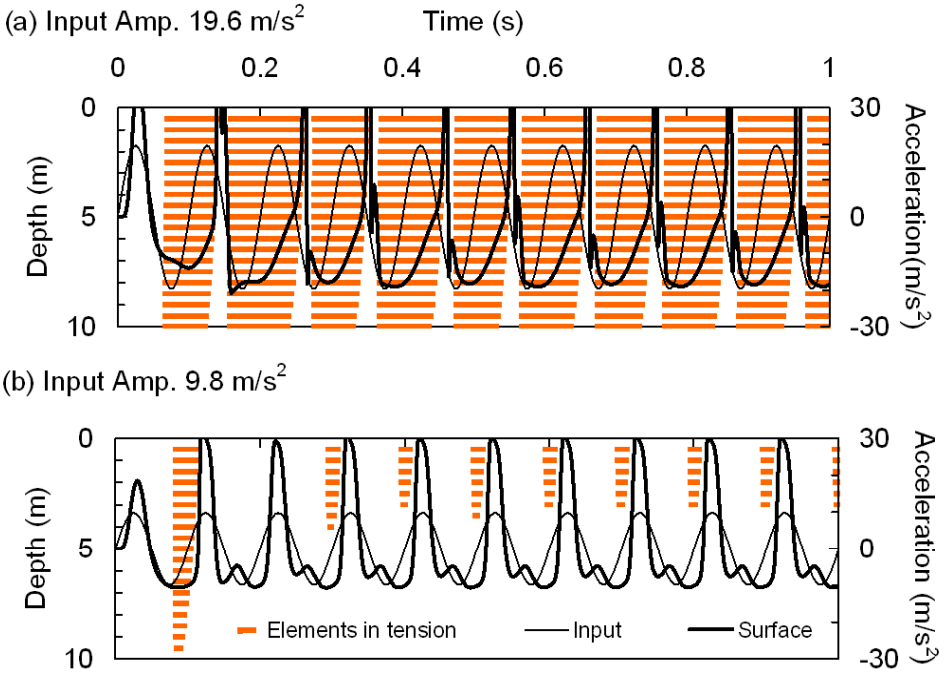

Figure 7. Time histories of input and surface accelerations (right axis) with horizontal bars indicating the duration of tension at the depth of each element (left axis).

PHYSICAL MODEL

A series of 1G shaking table tests were carried out with dry sands in a container whose dimension is 1.8 × 1.2 × 0.6 m^3 (Fig. 8). Upon constructing the uniform sand layer with 1.0 m thickness, a silica sand was air-pluviated and well compacted layer by layer so that the relative density was nearly 100%. Seven accelerometers and two laser displacement sensors were installed in the model ground (Fig. 8). Vertical sweep waves whose amplitude was 100 gals and frequency varied from 0 to 30 Hz were, firstly, input to check the natural frequency of the model ground, and it was determined as 12.4 Hz. Then, sinusoidal waves whose frequency range was 0.25 Hz to 50 Hz were vertically input. For each input frequency, the amplitude of the input acceleration was varied step by step from small (min. 50 gal) to large (max. 1,200 gal) amplitude, depending on the condition with which asymmetric vertical motion is reproduced.

As an example, Figure 9 shows recorded time histories of acceleration of 2 cases: Fig. 9(a) for the input motion of 10 Hz, 700 gal and Fig. 9(b) for 50 Hz, 200 gal. As it is clearly shown in the case of low frequency [Fig. 9(a)], asymmetric waveform can be reproduced in depth where accelerometers were installed (Fig. 8). For the case of higher frequency [Fig. 9(b)], the asymmetry is only seen in the record of surface acceleration. In both cases, as approaching to the surface, positive peak values become large, while negative peak values are kept almost the same in all depths. The waveform of the computed surface vertical acceleration (Fig. 8) is significantly similar to the one obtained from experiments (Fig. 9). This similarity may validate the use of numerical method adapted in this study.

Figure 10 summarizes the series of experiments in terms of input amplitude and frequency. In Fig. 10, solid circles indicate the cases in which asymmetric surface acceleration was observed, and those markers show that, as input frequency increases, the asymmetric waveform can be reproduced at smaller input amplitudes.

Figure 10(b) shows the relationship between the input acceleration amplitude and amplification factors. Here, the amplification factor is computed as a ratio of the maximum surface acceleration to the maximum input acceleration. A curve in Fig 10(b) indicates a borderline above which asymmetric waveforms are observed. When the asymmetric waveform is observed, the amplification factors of input acceleration with higher frequencies are larger than the ones of lower frequencies. For example, at 50 Hz, the maximum amplification factor is about 12 with the amplitude of 200 gal, while at 2.5 Hz, the maximum amplification factor is 2.5 with that of 1,000 gal.

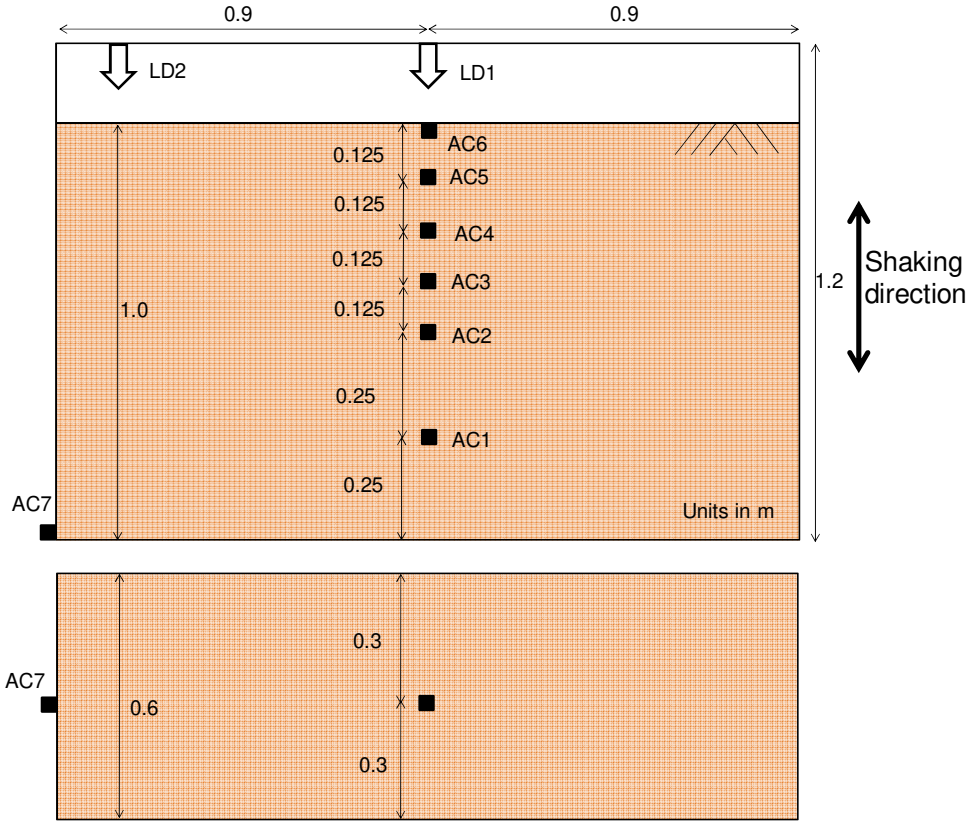

Figure 8. Location of accelerometers (AC1-AC7) and laser displacement transducers (LD1 and LD2) in 1G model test setup.

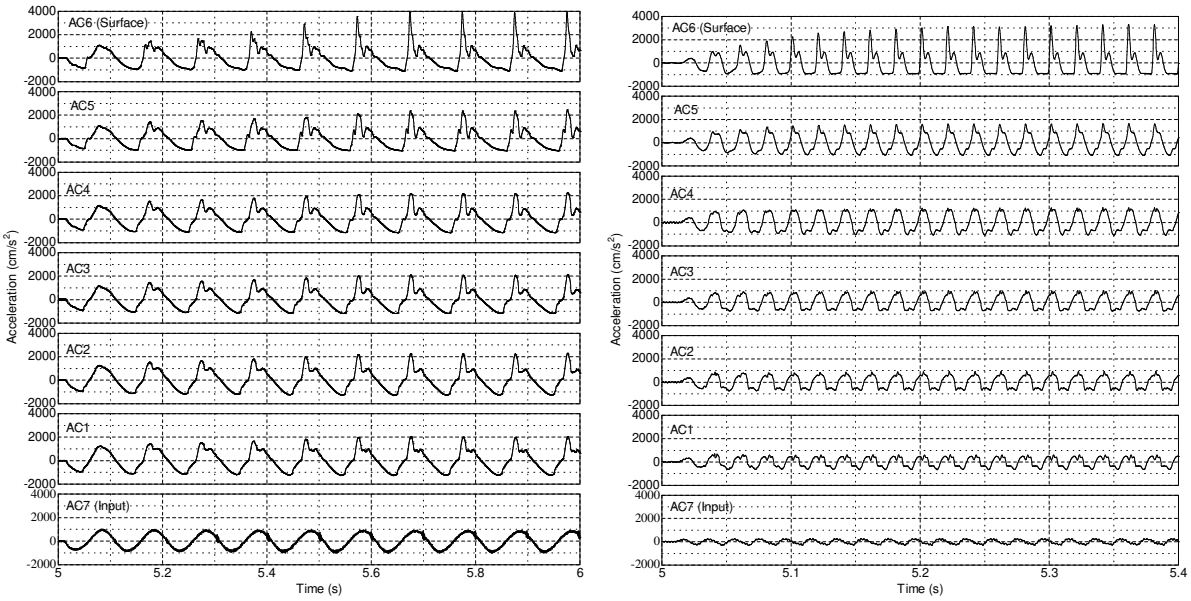

(a)10Hz, 700 gal (b) 50 Hz, 200 gal

Figure 9. Observed time histories of acceleration: (a) 10Hz, 700 gal, (b) 50 Hz, 200 gal.

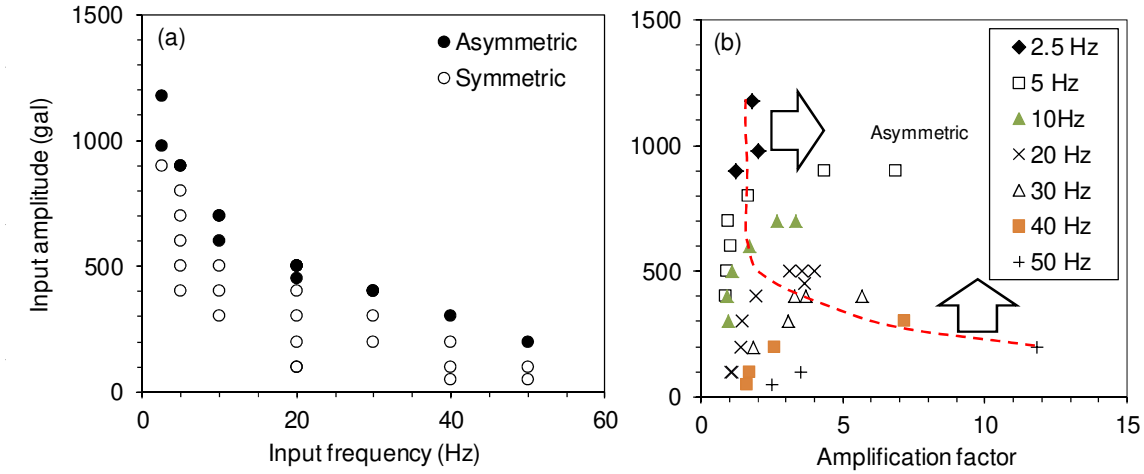

Figure 10. Summary of test cases: (a) input amplitude versus input frequency, (b) input amplitude versus amplification factor (max. surface acc. /max. input acc.)

CONCLUSIONS

During the 2008 Iwate-Miyagi Nairiku, Japan, earthquake, a very large acceleration record, which exceeded 40 m/s^2 (three components combined), was observed at the vertical array site, KiK-net, IWTH25 station. The surface vertical acceleration record had asymmetric amplitude. Tobita et al. (2010) conducted the numerical study and their results are partially presented in this paper. In addition to what they have reported, results from the 1 g model tests of the ground response against vertical motion were presented.

First, the observed asymmetric ground motion was simulated with a model ground of a column whose model parameters were derived from the borehole profile at the vertical array, KiK–net, IWTH25 site. Vertical acceleration at the surface clearly showed asymmetric form, as can be seen in the observed acceleration.

Then, response against vertical motion was studied with a simple column mesh with 10 m depth and a sinusoidal input motion of 10 Hz. When the amplitude of input acceleration was +/-2 g, tensile volumetric strains were generated as deep as 10 m, and the duration of tension was much longer than compression. On the other hand, if the amplitude of input acceleration was 1 g, the duration of tension was much shorter, and only the elements shallower than G.L. – 4 m fell in the tensile state. The analytical results indicated that the asymmetry in vertical surface acceleration might be characterized by the positive pulse due to compression stress applied to the ground material and the existence of a lower bound of negative acceleration, which in most cases corresponds to the acceleration of gravity.

In addition to the numerical analysis, physical model testing was carried out and their results were briefly introduced. The experiments was done with dry sand whose depth was 1 m. Seven accelerometers and 2 laser displacement transducers were attached to the model container. Vertical sinusoidal waves with various frequencies and amplitudes, and the recorded acceleration at the KiK-net site were input. The asymmetric waveforms were observed at a certain combination of input frequency and amplitude. Observed asymmetric waveform was significantly similar to the ones obtained from the numerical analysis conducted by the presented study. This validates the numerical model adapted in this study, FLIP.

Physical model tests conducted in the present study used dry sands which was somehow comparable to the assumption made in the numerical analysis. However, in reality, conditions of the natural ground can be much more complex; such as existence/combinations of ground water, cohesive soils and/or soft rocks. For better understanding of the effects of near field strong motions, dynamic behavior of such a ground under large vertical strong motions is yet to be investigated.

AKNOWLEDGEMENTS

The "Strong Earthquake Response Simulator (SERS)" operated by the Disaster Prevention Research Institute of Kyoto University was used for the 1 g model testing. The operation of facility is partially supported by the "Open Advanced Research Facilities Initiative" program by the Ministry of Education, Culture, Sports, Science and Technology (MEXT).

REFERENCES

Aoi, S., T. Kunugi and H. Fujiwara (2008). Trampoline effect in extreme ground motion, Science, 322, 727-730.

Bardet, J. P. and C. A. Davis (1996). Performance of San Fernando dams during the 1994 Northridge Earthquake, Journal of Geotechnical Engineering, ASCE, 122, 554-564.

Bonilla, L., Fabian, R. Archuleta, J. and D. Lavallee (2005). Hysteretic and dilatant behavior of cohesionless soils and their effects on nonlinear site response: Field data observations and modeling, Bulletin of the Seismological Society of America, 95, 2373-2395.

Eisler, J. and F. Chilton (1964). Spalling of the Earth's surface by underground nuclear explosions, Journal of Geophysical Research, 69, 5285-5293.

Frankel, A. D., D. L. Carver and R. A. Williams (2002). Nonlinear and linear site response and basin effects in Seattle for the M 6.8 Nisqually, Washington earthquake, Bulletin of the Seismological Society of America, 92, 2090-2109.

Holzer, T. L., T. L. Youd and T. C. Hanks (1989). Dynamic liquefaction during the 1987 Superstition Hills, California, earthquake, Science, 244 56-59.

Iai, S., Y. Matsunaga and T. Kameoka (1992). Strain space plasticity model for cyclic mobility, Soils and Foundations, Japanese Society of Soil Mechanics and Foundation Engineering, 32, 1- 15.

Iai, S., T. Morita, T. Kameoka, Y. Matsunaga and K. Abiko (1995). Response of a dense sand deposit during 1993 Kushiro-oki earthquake, Soils and Foundations, 35, 115-131.

Idriss, I. M. and H. B. Seed (1968). Analysis of ground motions during the 1957 San Francisco earthquake, Bulletin of the Seismological Society of America, 58, 2013-2032.

Idriss, I. M. (1990). Response of soft soil sites during earthquakes, Proceedings of the H. Bolton Seed Memorial Symposium, Vol. 2, J. M. Duncan (Editor), BiTech Publisher, Vancouver, 273-289.

Iwasaki, Y. and M. Tai (1996). Strong motion records at Kobe Port Island, Special Issue of Soils and Foundations, Japanese Geotechnical Society, 29-40.

Kayan, R., S. Brandenberg, J., B. Collins, D., S. Dickenson, S. Ashford, Y. Kawamata, Y. Tanaka, H. Koumoto, N. Abrahamson, L. Cluff and K. Tokimatsu (2009). Geoengineering and seismological aspects of the Niigata-Ken Chuetsu-Oki earthquake of 16 July 2007, Earthquake Spectra, 25, 777-802.

NIED (2010). Borehole profile of the Ichinoseki Nishi Station (IWTH25), http://www.kik.bosai.go.jp/kik/.

Towhata, I. and K. Ishihara (1985). Modelling soil behaviour under principal stress axes rotation, Proceedings of 5th International Conference on Numerical Methods in Geomechanics, Nagoya, Vol. 1, 523-530.

Tobita, T. Iai, S. and Iwata, T. (2010). Numerical analysis of near-field asymmetric vertical motion, Bulletin of Seismological Society of America, Vol. 100, No. 4, pp. 1456-1469.

Toyota, H. (2009). Personal communication.

Yamada, M., J. Mori and T. Heaton (2009). The slapdown phase in high-acceleration records of large earthquakes, Seismological Research Letters, 80, 559-564.